Performance Analysis and Location Optimization for Massive MIMO Systems with Circularly Distributed Antennas

Ang Yang, Yindi Jing, *Member, IEEE,* Chengwen Xing, *Member, IEEE,*

Zesong Fei, *Member, IEEE,* Jingming Kuang

Abstract

In this paper, we analyze the achievable rate of the uplink of a single-cell multi-user distributed massive multiple-input-multiple-output (MIMO) system. The multiple users are equipped with single antenna and the base station (BS) is equipped with a large number of distributed antennas. We derive an analytical expression for the asymptotic ergodic achievable rate of the system under zero-forcing (ZF) detector. In particular, we consider circular antenna array, where the distributed BS antennas are located evenly on a circle, and derive an analytical expression and closed-form tight bounds for the achievable rate of an arbitrarily located user. Subsequently, closed-form bounds on the average achievable rate per user are obtained under the assumption that the users are uniformly located in the cell. Based on the bounds, we can understand the behavior of the system rate with respect to different parameters and find the optimal location of the circular BS antenna array that maximizes the average rate. Numerical results are provided to assess our analytical results and examine the impact of the number and the location of the BS antennas, the transmit power, and the path-loss exponent on system performance. It is shown that circularly distributed massive MIMO system largely outperforms centralized massive MIMO system.

A. Yang, C. Xing, Z. Fei, and J. Kuang are with the School of Information and Electronics, Beijing Institute of Technology, Beijing, China. (Email: taylorkingyang@163.com, chengwenxing@ieee.org, feizesong@bit.edu.cn, JMKuang@bit.edu.cn).

Y. Jing is with the Department of Electrical and Computer Engineering, University of Alberta, Edmonton, AB, T6G 2V4 Canada (e-mail: yindi@ualberta.ca).

Index Terms

Massive MIMO, distributed MIMO, achievable rate analysis, antenna location optimization.

I. INTRODUCTION

With the demands of the wireless data services nowadays, high spectrum efficiency or data rate is undoubtedly an important feature of future wireless systems [1], [2]. In order to improve the data rate of wireless systems, various innovative ideas have been proposed and investigated. Among the most successful ones in recently years is the multiple-input-multiple-output (MIMO) concept [3], [4].

Recently, distributed MIMO systems, or distributed antenna systems, was proposed to further improve the data rate, in which multiple transmit or receive antennas are distributively located to reduce the physical transmission distance between the transmitter and the receiver [5]–[14]. The distributive antennas are assumed to be connected to the central unit via high-bandwidth and low-delay backhaul such as optical fiber channels. It has been proved that distributed MIMO outperforms centralized MIMO in outage probability and achievable rate. In [9], for a single-cell single-user distribute MIMO system with arbitrary antenna topology, the authors analyzed the outage performance as well as the diversity and multiplexing gains. For a single-cell distributed MIMO systems with multiple uniformly distributed users, upper bounds on the ergodic capacity of one user and approximate expressions of sum capacity of the cell were derived in [10]. In [11], both single-cell and two-cell distributed MIMO systems with multiple uniformly distributed users per cell are considered. The cells are assumed to be circular and the distributed base station (BS) antennas have circular layout. The locations of the distributive antennas were optimized to maximize lower bounds on the expected signal to noise ratio (SNR) and signal to leakage ratio. The resource (including power, subcarrier, and bit) allocation problems in single-cell multi-user distributed antenna systems were investigated in [12]. In [13], different radio resource management schemes were compared for multi-cell multi-user distributed antenna systems. In [14], for multi-cell networks with multiple remote antennas and one multi-antenna user in each

cell, the input covariances for all users were jointly optimized to maximize the achievable ergodic sum rate.

In the above literature of distributed MIMO, single user or multiple users with orthogonal channels are assumed, so there is no inter-user interference. However in current and future wireless systems, it is expected to have multiple users sharing the same time-frequency resource. In such systems, one user will suffer from the interferences of other users in the cell, which can largely degrade the system rate. To conquer the intra-cell user interference problem, the concept of massive MIMO, where the BS is equipped with a very large number of antennas usually of hundreds or higher, was proposed and attracted considerable attention recently [2], [15]–[26]. With a large number of antennas at the BS, according to the law of very long vectors, transmission channels for different users are orthogonal to each other. User-interference diminishes and very high data rate can be achieved with low complexity signal processing. The ergodic achievable rates of the single-cell multi-user massive MIMO uplink with linear detectors, i.e. maximum ratio combining (MRC), zero-forcing (ZF), minimum-mean-square-error (MMSE), have been derived in [20]. The achievable rates of both the uplink and downlink of multi-cell multi-user massive MIMO systems with linear precoders and detectors were analyzed in [21].

As the combination of the two promising concepts, massive MIMO and distributed MIMO, distributed massive MIMO systems are of great potential in fulfilling the increasing demands of next generation communication systems [27]–[31]. The authors in [27] focused on an uplink massive MIMO system consisting of multiple users and one BS with several large scale distributed antenna sets. In this system, the deterministic equivalence of the ergodic sum rate was derived and an iterative waterfilling algorithm was proposed for finding the capacity-achieving input covariance matrices. [28] analyzed the sum rates of distributed MIMO systems, in which L multiple-antenna radio ports form a virtual transmitter and jointly transmit data to a centralized multiple-antenna BS. The capacity and spatial degrees of freedom of a large distributed MIMO system were investigated in [29], where wireless users with single transmit and receive antenna cooperate in clusters to form distributed transmit and receive antenna arrays. In [30], a simplistic

matched filtering scheme and a subspace projection filtering scheme were investigated in a fixed size single-cell network, where the BS antennas are assumed uniformly and randomly located in the cell serving single-antenna users. In [31], for networks where one large-scale distributed BS with a grid antenna layout serving single-antenna users, the energy efficiency maximization problem was formulated under per-antenna transmit power and per-user rate constraints. low complexity channel-gain-based antenna selection method and interference-based user clustering method were proposed to improve the system energy efficiency.

In this paper, we consider the uplink of a single-cell multi-user distributed massive MIMO system in which the BS equipped with a large number of distributed antennas receives information from multiple single-antenna users. The asymptotic system achievable rate under linear ZF detector is analyzed for arbitrary but known antenna locations and for circular antenna layout. Based on the analysis, the location of the distributed antennas for circular antenna layout is optimized. Compared to [27], [28], the topology of the distributed BS antennas used in our work is different, as the BS in [27] is the combination of several centralized BS and the BS in [28] is centralized. Compared to [29], the transmitters in this work are non-cooperative single-antenna users, while the users in [29] cooperate with each other and form a virtual transmitter with distributed antenna arrays. Thus our system model and derivations of achievable rate are different from [27]–[29]. Compared to [30], [31], we focus on the derivations of achievable rate and the location optimization of the distributive BS antennas, while [30] faces the problem of interference control through the use of second-order channel statistics and [31] works on the energy efficiency maximization problem. The major contributions of this paper are summarized as follows.

- We provide new results for independent but non-identically distributed (i.n.i.d) random vectors with very high dimension (see Lemma 1). Based on the results, an analytical expression for the asymptotic achievable rate of multi-user distributed massive MIMO systems is derived for arbitrary but known user location and antenna deployment (see Proposition 1).

- We consider a practical circular antenna layout, where antennas of the BS are located evenly in a circle. The asymptotic achievable rates for an arbitrarily located user and two closed-form tight bounds are derived (see Theorems 1 and 2).

- Furthermore, for the circular antenna layout, tight closed-form bounds on the average rate of the cell with uniform user location are obtained (see Theorem 3). These results can be used to predict the system performance and understand its behavior with respect to the number of antennas, the location of antenna, the cell size, and the transmit power.

- Based on the acquired tight bounds, we derive the optimal radius of the distributed antennas for the maximum average achievable rate (see Lemma 2), which guides the fundamental and practical problem of antenna placement for distributed MIMO systems.

- Finally, numerical results are provided to assess our analysis. It is shown that multi-user distributed massive MIMO is largely superior to centralized massive MIMO in achievable uplink rate.

The remaining of the paper is organized as follows. The system model and asymptotic achievable rate analysis of a general distributed massive MIMO system are presented in Section II. Asymptotic achievable rate analysis of the circularly distributed massive MIMO is present in Section III. Location optimization of the circularly distributed antennas is provided in Section IV. Simulation results are presented in Section V. Conclusions are drawn in Section VI. Involved proofs are included in the appendices.

Notation: Boldface lowercase letters denote vectors, while boldface uppercase letters denote matrices. We use $(\cdot)^{\mathrm{T}}$, $(\cdot)^{*}$ and $(\cdot)^{\mathrm{H}}$ to denote the transpose, conjugate and conjugate transpose of a matrix or a vector, respectively. For a matrix $\mathbf{Z}$, $\mathrm{Tr}(\mathbf{Z})$ is its trace. The symbol $\mathbf{I}_M$ denotes the $M \times M$ identity matrix, while $\mathbf{0}_{M,N}$ denotes the $M \times N$ matrix whose entries are zeros. The symbol $\mathbb{E}$ denotes the statistical expectation operation. The symbol $\|\cdot\|_F$ denotes Frobenius norm of a matrix or a vector. The function $\log_2(\cdot)$ is the base-2 logarithm and $\ln(\cdot)$ is the natural logarithm.
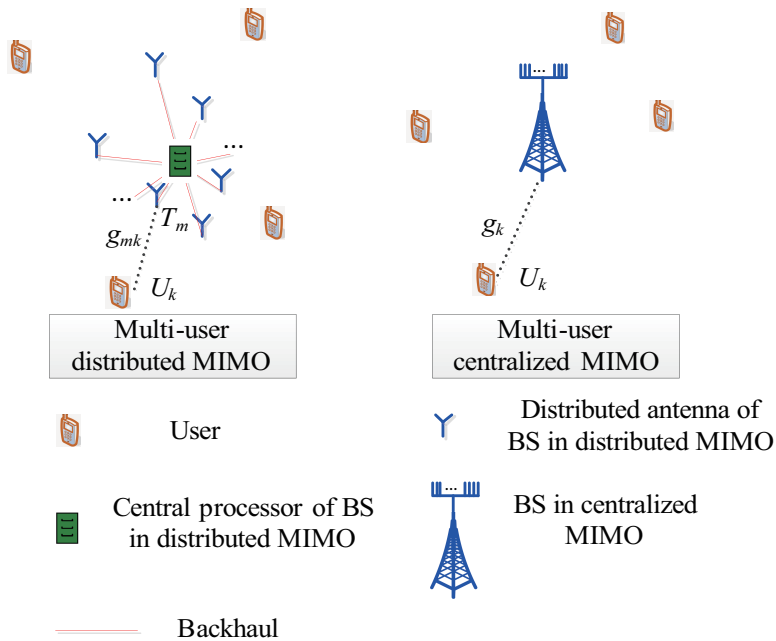
Fig. 1. System models of multi-user distributed MIMO (left side) and multi-user centralized MIMO (right side).

II. SYSTEM MODEL AND ASYMPTOTIC ACHIEVABLE RATE ANALYSIS

A. Multi-User Distributed Massive MIMO System Model

We consider a single-cell multi-user distributed massive MIMO system. As shown in the left side of Figure 1, in this system, there is one BS equipped with M antennas which are spatially distributed [30], [31]. The number of antennas M is assumed to be large, e.g., a few hundreds. This is different to the multi-user centralized MIMO system [15]–[26], where the BS antennas are centralized and spatially co-located (shown in the right side of Figure 1). Compared with centralized MIMO systems, distributed MIMO systems provide macro-diversity and have enhanced network coverage and capacity, due to their open and flexible infrastructure [6], [7], [27]. We assume that the distributed BS antennas are connected with high capacity backhaul and have ideal cooperation with each other. There are K users, each equipped with single antenna. We assume that $M \gg K$.

Denote the channel coefficient between the mth antenna of the BS and the kth user as g_{mk}.

We consider both the path-loss and small-scale fading as follows [31]

$$g_{mk} = h_{mk}\sqrt{\beta_{mk}}, \quad m = 1, 2, \ldots, M, \ k = 1, 2, \ldots, K, \tag{1}$$

where h_{mk} is the small-scale fading coefficient, which is model as a random variables with zero-mean and unit-variance. Without loss of generality, Rayleigh fading is adopted in the simulation, where h_{mk} follows circularly symmetric complex Gaussian (CSCG) distribution, i.e., $h_{mk} \sim \mathcal{CN}(0, 1)$. h_{mk}'s are assumed to be mutually independent. β_{mk} models the path-loss. We assume that

$$\beta_{mk} = d_{mk}^{-v}, \tag{2}$$

where d_{mk} is the distance between mth antenna of the BS and the kth user and v is the path-loss exponent with typical values ranging from 2 to 6, i.e., $2 \leq \nu \leq 6$. Let

$$\mathbf{g}_k \triangleq \begin{bmatrix} g_{1k} & \cdots & g_{Mk} \end{bmatrix}^{\mathrm{T}},$$

which is the $M \times 1$ channel vector between kth user and all M BS antennas. Let

$$\mathbf{G} \triangleq \begin{bmatrix} \mathbf{g}_1 & \cdots & \mathbf{g}_K \end{bmatrix},$$

which is the channel matrix between all K users and all M BS antennas. Perfect channel state information (CSI) is assumed at the BS, that is, the BS knows $\mathbf{G}$ precisely.

The uplink communication is studied, where the K users transmit their data in the same time-frequency resource to the BS. Let $\mathbf{x}$ be the $K \times 1$ signal vector containing the user data, where its k-th entry x_k is the information symbol of the kth user. $\mathbf{x}$ is normalized as $\mathbb{E}\{\|\mathbf{x}\|_F^2\} = 1$. Let P be the average transmit power of each user. This implies that in this work, we assume that all users have the same transmit power. But the derived results can be directly employed to non-equal power case. The $M \times 1$ vector of the received signals at the BS is

$$\mathbf{y} = \sqrt{P}\mathbf{G}\mathbf{x} + \mathbf{n}, \tag{3}$$

where $\mathbf{n}$ is the noise vector, whose entries are assumed to be independent and identically distributed (i.i.d.) CSCG random variables with zero-mean and unit-variance, that is, $\mathbf{n} \sim \mathcal{CN}(\mathbf{0}, \mathbf{I}_M)$.

ZF linear detector is used at the receiver, which has low-complexity and achieves comparable sum-rate performance to other more complicated designs such as the minimum-mean-square-error (MMSE) detector in massive MIMO systems [20], [21]. ZF separates data streams from different users by multiplying the received signal vector $\mathbf{y}$ with $\mathbf{A} \triangleq \left(\mathbf{G}^H \mathbf{G}\right)^{-1} \mathbf{G}^H$. From (3), we have

$$\mathbf{r} = \mathbf{A}\mathbf{y} = \left(\mathbf{G}^H \mathbf{G}\right)^{-1} \mathbf{G}^H \mathbf{y} = \sqrt{P}\mathbf{x} + \left(\mathbf{G}^H \mathbf{G}\right)^{-1} \mathbf{G}^H \mathbf{n}. \tag{4}$$

Focusing on the kth element of $\mathbf{r}$, we have, from (4),

$$r_k = \sqrt{P}x_k + \mathbf{a}_k^H \mathbf{n}, \tag{5}$$

where $\mathbf{a}_k$ is the kth column of the matrix $\mathbf{A}$. Since $\mathbf{n} \sim \mathcal{CN}(\mathbf{0}_{M \times 1}, \mathbf{I}_M)$, the equivalent noise $\mathbf{a}_k^H \mathbf{n}$ is a CSCG random variable with zero mean and variance $\|\mathbf{a}_k\|_F^2$, i.e., $\mathbf{a}_k^H \mathbf{n} \sim \mathcal{CN}(0, \|\mathbf{a}_k\|_F^2)$. There is no interference term in (5) due to the ZF matrix structure. It is noteworthy that ZF detector is chosen here for the simplicity of the presentation and our work can be straightforwardly extended to MMSE linear detector.

B. Asymptotic Achievable Rate Analysis

In this subsection, we analyze the asymptotic achievable rate of the multi-user distributed massive MIMO uplink when $M \to \infty$, for a general BS antenna deployment and user location.

To assist the analysis, we first prove the following results for very long random vectors.

Lemma 1. *Let* $\mathbf{p} \triangleq \begin{bmatrix} p_1 & p_2 & \dots & p_M \end{bmatrix}^T$ *and* $\mathbf{q} \triangleq \begin{bmatrix} q_1 & q_2 & \dots & q_M \end{bmatrix}^T$ *be independent* $M \times 1$ *vectors whose elements are i.n.i.d. zero-mean random variables. Assume that* $\mathbb{E}\left\{|p_i|^2\right\} = \sigma_{p,i}^2$, $\mathbb{E}\left\{|p_i|^4\right\} < \infty$ *and* $\mathbb{E}\left\{|q_i|^2\right\} = \sigma_{q,i}^2$, $\mathbb{E}\left\{|q_i|^4\right\} < \infty$ *for* $i = 1, 2, \dots, n$. *We have, when* $M \to \infty$,

$$\frac{1}{M}\mathbf{p}^H \mathbf{p} \xrightarrow{a.s.} \frac{1}{M}\sum_{i=1}^{M} \sigma_{p,i}^2, \tag{6}$$

and

$$\frac{1}{M}\mathbf{p}^H \mathbf{q} \xrightarrow{a.s.} 0, \tag{7}$$

where $\overset{a.s.}{\to}$ denotes the almost sure convergence.

Proof: See Appendix A. ∎

The results in Lemma 1 can be seen as generalizations of the results in Eqs. (4) and (5) in [20]. More specifically, the results in [20] are for very long random vectors with i.i.d. elements, while the results in Lemma 1 can be applied to very long random vectors with i.n.i.d. elements.

With the results in Lemma 1, we can obtain the following expression for the asymptotic achievable rate of distributed massive MIMO systems.

Proposition 1. *When $M \to \infty$, the average achievable rate of the kth user in the multi-user distributed MIMO system has the following asymptotic behavior:*

$$R_k \overset{a.s.}{\to} \log_2 \left(1 + P \sum_{m=1}^{M} \beta_{mk} \right). \tag{8}$$

Proof: From (5), the ergodic achievable rate of the kth user is

$$R_k = \mathbb{E} \left\{ \log_2 \left(1 + \frac{P}{\|\mathbf{a}_k\|^2} \right) \right\} = \mathbb{E} \left\{ \log_2 \left(1 + \frac{P}{\left[(\mathbf{G}^H \mathbf{G})^{-1} \right]_{kk}} \right) \right\}. \tag{9}$$

From Lemma 1, when $M \to \infty$, we have

$$\frac{1}{M} \|\mathbf{g}_k\|^2 \overset{a.s.}{\to} \frac{1}{M} \sum_{i=1}^{M} \mathbb{E} \left\{ |g_{ik}|^2 \right\} = \frac{1}{M} \sum_{i=1}^{M} \beta_{ik}, \tag{10}$$

$$\frac{1}{M} \mathbf{g}_k^H \mathbf{g}_i \overset{a.s.}{\to} 0, i \neq k. \tag{11}$$

Entries of $\left(\mathbf{G}^H \mathbf{G} \right)^{-1}$ are continuous and have finite first order derivatives with respect to $\mathbf{g}_1, \mathbf{g}_2, \ldots, \mathbf{g}_K$ when $\mathbf{G}$ is non-singular. Meanwhile, the probability of $\mathbf{G}$ is singular is zero. Thus, we have

$$\left(\mathbf{G}^H \mathbf{G} \right)^{-1} = \frac{1}{M} \left(\frac{1}{M} \mathbf{G}^H \mathbf{G} \right)^{-1}$$

$$\overset{a.s}{\to} \frac{1}{M} \mathrm{diag} \left\{ \frac{\sum_{i=1}^{M} \beta_{i1}}{M}, \frac{\sum_{i=1}^{M} \beta_{i2}}{M}, \frac{\sum_{i=1}^{M} \beta_{iK}}{M} \right\}^{-1}$$

$$= \mathrm{diag} \left\{ \sum_{i=1}^{M} \beta_{i1}, \sum_{i=1}^{M} \beta_{i2}, \sum_{i=1}^{M} \beta_{iK} \right\}^{-1} \tag{12}$$

By substituting (12) into (9), the proposition is proved. ∎

The result in Eq. (8) of Proposition 1 can be applied to massive MIMO systems with arbitrary antenna deployment and user location. Proposition 1 is also applicable to MMSE detector, where $\mathbf{A} = \left(\mathbf{G}^H\mathbf{G} + \frac{1}{P}\mathbf{I}_k\right)^{-1}\mathbf{G}^H$. With the MMSE detector, we can change Eqs. (4), (5), and (9) accordingly to include the interference. But due to the large number of antennas, the interference term will diminish and the same achievable rate result can be obtained.

The multi-user centralized MIMO system considered in [15], [20]–[22] can be seen as a special case of our multi-user distributed MIMO system with all the distributed antennas located in the same place, i.e., $\beta_{mk} = \beta_k$ for the kth user. Thus, from (8), we can obtain its achievable rate result as

$$R_{k,\text{central}} \overset{a.s.}{\to} \log_2\left(1 + PM\beta_k\right), \tag{13}$$

which is the same as Eq. (13) in [20].

III. ASYMPTOTIC ANALYSIS FOR THE ACHIEVABLE RATE OF CIRCULARLY DISTRIBUTED ANTENNAS

Theoretically speaking, antennas in a distributed massive MIMO system can take arbitrary locations and topology. The optimization of the antenna locations can be highly challenging, if not intractable, due to the large number of antennas and design parameters. On the other hand, arbitrary antenna locations or optimal topology may have prohibitive backhaul cost and installation cost. In real applications, it is more practical to consider manageable antenna topology. In this work, we consider circularly located BS antennas, where all antennas are on a circle centered at the cell enter. Circular topology has ideal symmetry and low dimension (radius and angle). Compared with the line topology, it is expected to have superior performance due to better symmetry. Compared with the grid topology, it is expected to have lower implementation cost and more tractability in analysis. Circular antenna layout has been considered in the literature [11], [32], [33] and shown to have good performance.

In this section, for distributed massive MIMO systems with circular antenna layout, we first specify the system model, then analyze the asymptotic achievable rate for an arbitrary user, and
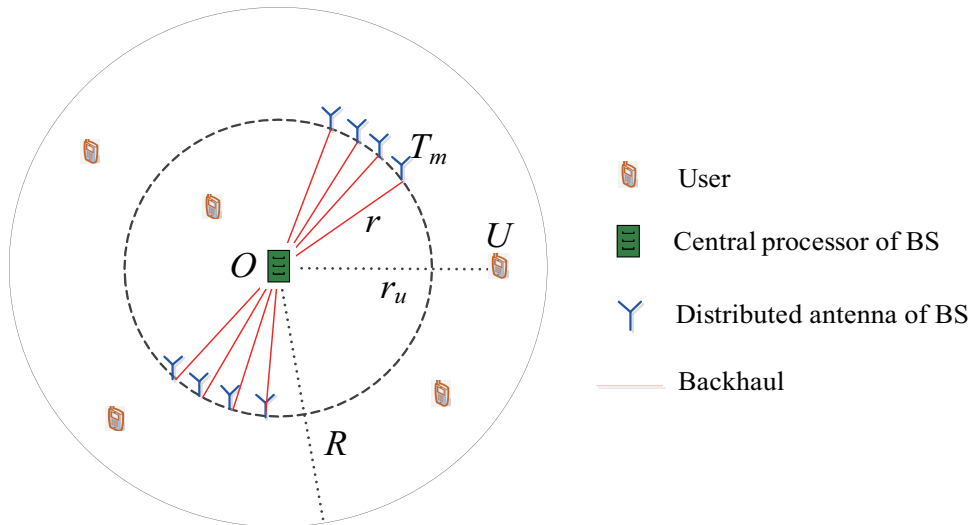
Fig. 2. Distributed massive MIMO system with circular BS antennas.

finally derive the average sum-rate per user assuming uniform user location.

The single-cell multi-user distributed massive MIMO system is shown in Figure 2. We consider a circular cell with radius R. The center of the cell is denoted as O. Circular cell is widely used [11], [32], [34] and has been shown to have similar performance to hexagonal cell. But it enjoys more tractable analysis. The distributed BS antennas are located evenly on a smaller circle with radius r, whose center is the same as the center of the cell. We denote the location of the mth BS antenna as T_m. Thus, the length of the segment OT_m is r. Notice that since the BS antennas are evenly located on the circle and the antenna number is assumed to be large, the angle dimension of the antenna location (for example, the angle of the segment OT_m and the horizontal axis) has little effect on the system performance and only the radius of the antenna circle matters. We denote the location of an arbitrarily user as U. Let r_u be the distance between the user and the cell center, i.e., the length of the segment OU.

A. *Asymptotic Achievable Rate of an Arbitrary User for Circularly Distributed Massive MIMO*

The following results on the asymptotic achievable rate of an arbitrary user at distance r_u for the circularly distributed massive MIMO system are obtained.

Theorem 1. *For the circularly distributed massive MIMO system with antenna radius r, when $M \to \infty$, the ergodic achievable rate of the user at distance r_u from the cell center has the following asymptotic behavior:*

$$R \overset{a.s.}{\to} R_{asy} \triangleq \log_2 \left(1 + PMI_0 \right), \tag{14}$$

where

$$I_0 \triangleq \left| r^2 - r_u^2 \right|^{-\frac{v}{2}} P_{\frac{v}{2}-1} \left(\frac{r^2 + r_u^2}{\left| r^2 - r_u^2 \right|} \right), \tag{15}$$

with $P_.(\cdot)$ the Legendre function [37].

For $\nu = 2, 4, 6$, closed-form expressions for the achievable rate can obtained as follows:

$$R \overset{a.s.}{\to} R_{asy} \triangleq \begin{cases} \log_2 \left(1 + PM \frac{1}{|r^2 - r_u^2|} \right), & \text{if } v = 2, \\ \log_2 \left(1 + PM \frac{r^2 + r_u^2}{|r^2 - r_u^2|^3} \right), & \text{if } v = 4, \\ \log_2 \left[1 + PM \cdot \frac{3 \left(\frac{r^2 + r_u^2}{r^2 - r_u^2} \right)^2 - 1}{2 |r^2 - r_u^2|^3} \right], & \text{if } v = 6. \end{cases} \tag{16}$$

Proof: See Appendix B. ∎

In this theorem, to facilitate the presentation, we introduce a new notation, R_{asy} for the asymptotic ergodic achievable rate of a user when $M \to \infty$. Note that $P_a(b) = F\left(-a, a+1; 1; \frac{1-b}{2} \right)$, where $F(\cdot, \cdot; \cdot; \cdot)$ is the Gauss hypergeometric function [37]. Many software for scientific computations such as Matlab have this function. Thus the result in (14) and (15) of Theorem 1 can be easily calculated numerically. However, due to the special function, for $\nu \neq 2, 4, 6$, the achievable rate is not in closed-form and little insight can be obtained on the performance behavior of the circularly distributed massive MIMO system with respect to the cell size and antenna location. Thus, in what follows, we derive bounds on the achievable rate in closed-form.

Theorem 2. *Define*

$$R^{B,1} \triangleq \log_2 \left(1 + PM \frac{(r_u^2 + r^2)^{\frac{v}{2}-1}}{|r_u^2 - r^2|^{v-1}} \right), \tag{17}$$

$$R^{B,2} \triangleq \log_2 \left(1 + PM \frac{(r_u^2 + r^2)^{\frac{v}{2}-1}}{|r_u^2 - r^2|^{v-1}} \cdot \frac{2^{3\left(\frac{v}{2}-1\right)} \Gamma^2 \left(\frac{v}{2} - \frac{1}{2} \right)}{\pi \Gamma(v-1)} \right). \tag{18}$$

For the circularly distributed massive MIMO system with antenna radius r, the asymptotic achievable rate of a user at distance r_u from the cell center, denoted as R_{asy}, can be bounded as follows

$$\begin{cases} R^{B,1} \geq R_{asy} \geq R^{B,2}, & \text{if } 2 \leq \nu \leq 4, \\ R^{B,1} \leq R_{asy} \leq R^{B,2}, & \text{if } 6 \geq \nu \geq 4, \\ R_{asy} = R^{B,1} = R^{B,2}, & \text{if } \nu = 2 \text{ or } 4. \end{cases} \tag{19}$$

Proof: See Appendix C. ■

Theorem 2 provides both lower and upper bounds on the achievable rate. When $v \geq 4$, $R^{B,1}$ is a lower bound and $R^{B,2}$ is an upper bound; when $v \leq 4$, $R^{B,1}$ is an upper bound and $R^{B,2}$ is a lower bound. When $\mu = 2, 4$, $R^{B,1}$ and $R^{B,2}$ are the same and equal the achievable rate of the user. Moreover, it is evident that the bounds in Theorem 2 are in closed-form. We note that the coefficient $\frac{2^{3\left(\frac{1}{2}v-1\right)}\Gamma^2\left(\frac{v}{2}-\frac{1}{2}\right)}{\pi\Gamma(v-1)}$ in (18) only depends on ν, the path-loss exponent and can be easily calculated offline.

To justify the tightness of the two closed-form bounds, we analyze their difference as follows:

$$\begin{aligned} \left|R^{B,1} - R^{B,2}\right| &= \left|\log_2 \frac{1 + PM\frac{\left(r_u^2+r^2\right)^{\frac{v}{2}-1}}{|r_u^2-r^2|^{v-1}}}{1 + PM\frac{\left(r_u^2+r^2\right)^{\frac{v}{2}-1}}{|r_u^2-r^2|^{v-1}} \cdot \frac{2^{3\left(\frac{v}{2}-1\right)}\Gamma^2\left(\frac{v}{2}-\frac{1}{2}\right)}{\pi\Gamma(v-1)}}\right| \\ &\leq \left|\log_2 \frac{2^{3\left(\frac{v}{2}-1\right)}\Gamma^2\left(\frac{v}{2}-\frac{1}{2}\right)}{\pi\Gamma(v-1)}\right| \overset{(a)}{<} 0.6, \end{aligned}$$

where (a) is obtained by software calculations for $2 \leq v \leq 6$. This shows that the two bounds are close to each other with less than 0.6 bits/s/Hz difference. The difference is negligible for massive MIMO systems as both bounds $R^{B,1}$ and $R^{B,2}$ increase in $\log_2 M$. Thus, either $R^{B,1}$ and $R^{B,2}$ can function as a tight closed-form approximation of the achievable rate when the number of BS antennas is large. Our simulation results in Section V also justify the tightness of the bounds.

Since both bounds $R^{B,1}$ and $R^{B,2}$ increase in $\log P$ where P is the transmit power and $\log M$ where M is the number of BS antennas, the user achievable rate is proved to increase in $\log P$ and $\log M$.

B. Asymptotic Average Achievable Rate of the Cell for Circularly Distributed Massive MIMO

In the previous subsection, we have analyzed the asymptotic rate of an arbitrarily located user in the cell. In this subsection, we derive the asymptotic average rate of a user in the cell, which indicates the average experience of user service. The users are assumed to be randomly and uniformly located [11], [36]. Thus, the probability distribution function of a user's distance to the cell center, denoted as r_u, is

$$f_{r_u}(x) = \frac{2}{R^2}x. \tag{20}$$

The angle of the user's location (to the horizonal axis) is uniform distributed on $[0, 2\pi)$. The following theorem on the asymptotic average rate of a user is proved.

Theorem 3. *Define*

$$\bar{R}^{B,1} = \log_2(PM) + \left(\frac{v}{2} - 1\right)\left(1 + \frac{r^2}{R^2}\right)\log_2\left(R^2 + r^2\right) - (v - 1)\left(1 - \frac{r^2}{R^2}\right)\log_2\left(R^2 - r^2\right)$$

$$- (3v - 4)\frac{r^2}{R^2}\log_2 r + \frac{v}{2}\log_2 e, \tag{21}$$

$$\bar{R}^{B,2} = \bar{R}^{B,1} + \log_2\frac{\Gamma^2\left(\frac{v}{2} - \frac{1}{2}\right)}{\pi\Gamma(v - 1)} + 3\left(\frac{v}{2} - 1\right). \tag{22}$$

For the circularly distributed massive MIMO system with uniformly distributed users in the cell, the asymptotic average achievable rate per user of the cell, denoted as $\bar{R}_{asy}$, can be bounded as follows:

$$\begin{cases} \bar{R}^{B,1} \gtrsim \bar{R}_{asy} \gtrsim \bar{R}^{B,2}, & if \ 2 \le v \le 4, \\ \bar{R}^{B,1} \lesssim \bar{R}_{asy} \lesssim \bar{R}^{B,2}, & if \ 6 \ge v \ge 4, \\ \bar{R}_{asy} \approx \bar{R}^{B,1} \approx \bar{R}^{B,2}, & if \ v = 2 \ or \ 4. \end{cases} \tag{23}$$

Proof: With uniformly distributed user location and the probability density function of the user distance to the cell center in (20), the asymptotic average achievable rate per user of the cell can be calculated as:

$$\bar{R}_{asy} = \frac{2}{R^2}\int_0^R r_u R_{asy}(r_u)d(r_u), \tag{24}$$

where $R_{asy}(r_u)$ is the asymptotic achievable rate for a user at distance r_u. From (19) in Theorem 2, we have (23), where

$$\bar{R}^{B,1} \triangleq \frac{2}{R^2} \int_0^R r_u R^{B,1}(r_u) dr_u, \quad \bar{R}^{B,2} \triangleq \frac{2}{R^2} \int_0^R r_u R^{B,2}(r_u) dr_u.$$

From (17) in Theorem 2, we have

$$\bar{R}^{B,1} = \frac{2}{R^2} \int_0^R r_u \log_2 \left(1 + PM \frac{(r_u^2 + r^2)^{\frac{v}{2}-1}}{|r_u^2 - r^2|^{v-1}} \right) dr_u \tag{25}$$

$$\approx \frac{2}{R^2} \int_0^R r_u \log_2 \left(PM \frac{(r_u^2 + r^2)^{\frac{v}{2}-1}}{|r_u^2 - r^2|^{v-1}} \right) dr_u \tag{26}$$

$$= \frac{\log_2 e}{R^2} \left[\int_0^{R^2} \ln(PM) \, dt + \left(\frac{v}{2} - 1 \right) \int_0^{R^2} \ln(t + r^2) \, dt \right. \tag{27}$$

$$\left. - (v-1) \int_0^{R^2} \ln \left| t - r^2 \right| dt \right]$$

$$= \log_2(PM) + \left(\frac{v}{2} - 1 \right) \log_2 e \left[\ln(R^2 + r^2) + \frac{r^2}{R^2} \ln \frac{R^2 + r^2}{r^2} - 1 \right]$$

$$- \frac{v-1}{R^2} \log_2 e \left[\int_0^{r^2} \ln(r^2 - t) dt + \int_{r^2}^{R^2} \ln(t - r^2) dt \right]$$

$$= \log_2(PM) + \left(\frac{v}{2} - 1 \right) \log_2 e \left(\ln(R^2 + r^2) + \frac{r^2}{R^2} \ln \frac{R^2 + r^2}{r^2} - 1 \right)$$

$$- (v-1) \log_2 e \left[\frac{r^2}{R^2} \ln r^2 + \left(1 - \frac{r^2}{R^2} \right) \ln(R^2 - r^2) - 1 \right],$$

from which we can obtain (21) via simple rewriting.

In deriving (26), we have used the approximation $\log(1 + x) \approx \log x$ for $x \gg 1$. When $M \gg 1$, we can see from (25) that the approximation applies. With straightforward and similar calculations, we can obtain (22). ∎

It is evident that our derived bounds on the asymptotic average achievable rate in Theorem 3 are in closed-form. Also, calculating the difference between the two bounds, we have

$$\left| \bar{R}^{B,1} - \bar{R}^{B,2} \right| = \left| \log_2 \frac{\Gamma^2 \left(\frac{v}{2} - \frac{1}{2} \right)}{\pi \Gamma(v-1)} + 3 \left(\frac{v}{2} - 1 \right) \right| < 0.6. \tag{28}$$

Thus, either bound can be used as a tight approximation of $\bar{R}_{asy}$ with the error being less than 0.6 bits/s/Hz. The error is negligible when $M \gg 1$ since $\bar{R}_{asy}$ increases in logarithm in M. The

tightness of the bounds will also be justified by our simulation results in Section V.

IV. Location Optimization of the Circular Antenna Array

In the previous section, the ergodic achievable rate of an arbitrarily located user and the average achievable rate per user of the cell for uniformly located users are derived when $M \to \infty$. We can see from the results that other than the transmit power P and the number of the distributive antennas M, the radius of the distributed antennas r largely affects the average achievable rate. In this section, we turn to derive the optimal radius of the circularly distributed antenna array to maximize the average achievable rate of the cell, which is one of the most important measures of wireless system performance.

In Theorem 3, both the upper and lower bounds, $\bar{R}^{B,1}$ and $\bar{R}^{B,2}$, are derived for the average achievable rate per user. The bounds are in closed-form and shown to be close to each other. Thus, in the radius optimization, we aim at maximizing $\bar{R}^{B,1}$. The same result can be obtained if $\bar{R}^{B,2}$ is used since the difference $\bar{R}^{B,2} - \bar{R}^{B,1}$ only depends on v and is independent of r, the radius of the circular antenna array.

Lemma 2. *The radius of the circular antenna array for the distributed massive MIMO system that maximizes $\bar{R}^{B,1}$ is:*

$$r_{opt} = \sqrt{\frac{R^2}{t_0 + 1}} \tag{29}$$

where t_0 is the solution of the following equation:

$$x^{3+\frac{2}{v-2}} + 2x^{2+\frac{2}{v-2}} - 1 = 0. \tag{30}$$

Proof: The derivative of $\bar{R}^{B,1}$ in (21) with respect to r can be calculated to be:

$$\frac{d\bar{R}^{B_1}}{dr} = \frac{r\log_2 e}{R^2} \left\{ (v-2)\ln\left(\frac{R^2}{r^2} + 1\right) + (2v-2)\ln\left(\frac{R^2}{r^2} - 1\right) \right\} \tag{31}$$

By making $d\bar{R}^{B_1}/dr$ zero, we have

$$\left(\frac{R^2}{r^2} + 1\right)^{\frac{v/2-1}{v-1}} \left(\frac{R^2}{r^2} - 1\right) = 1. \tag{32}$$

After replacing $R^2/r^2 - 1$ with t and rearranging the expression in (32), we obtain (30).

Next we show that the solution of (32), denoted as r_{opt}, is the maximum of $\bar{R}^{B_1}$. From (31), we can see that $\left(\frac{r\log_2 e}{R^2}\right)^{-1}\frac{d\bar{R}^{B_1}}{dr}$ is a decreasing function of r. Thus we have $\left(\frac{r\log_2 e}{R^2}\right)^{-1}\frac{d\bar{R}^{B_1}}{dr} > 0$ when $r < r_{opt}$ and $\left(\frac{r\log_2 e}{R^2}\right)^{-1}\frac{d\bar{R}^{B_1}}{dr} < 0$ when $r > r_{opt}$. Notice that $\frac{r\log_2 e}{R^2} > 0$. Thus we have $d\bar{R}^{B_1}/dr > 0$ when $r < r_{opt}$ and $d\bar{R}^{B_1}/dr < 0$ when $r > r_{opt}$. This ends the proof. ∎

The equation in (30) only depends on the path-loss exponent v and can be easily solved offline by many softwares such as Matlab. Using the result in Lemma 2, the radius of the distributed circular BS antenna array can be designed for the maximum average achievable rate for the distributed massive MIMO system.

From (29) we have $r_{opt}/R = 1/\sqrt{t_0 + 1}$. Thus, the ratio of the antenna radius and the cell radius depends on the path-loss exponent v only and is independent of the transmit power P and the BS antennas size M. This is very appealing in wireless network designs and implementation. Based on this fact, we further note that the improvement of the hardware in distributed MIMO, such as increasing the number of the distributed antennas, will not affect the optimal location of the distributive antennas.

V. NUMERICAL RESULTS

In this section, we present numerical results to show the performance of the distributed massive MIMO system with circular BS antenna array and justify the accuracy of our theoretical results. The impacts of different parameters, such as the number and the location of the distributive antennas, the transmit power, and the path-loss exponent, on the achievable rate are also investigated. We consider the uplink of a circular cell whose cell radius is set as $R = 1000$ meters. There is a massive BS with M circularly distributed antennas located on a circle of radius r. There are $K = 9$ users. The users have the same transmit power, which is set to be $P \times r_{mid}^v$ where $r_{mid} = R/2 = 500$ meters. So, if a user is located 500 meters away from a BS antenna, the average received SNR of the antenna from the user is P. The normalization with r_{mid}^v in the transmit power does not affect the behavior of the simulation curves but only affects

the position of the curves on the P axis. The small-scale channel fading h_{mk} is generated as circularly symmetric complex Gaussian with zero-mean and unit-variance, thus Rayleigh fading.

A. Achievable Rate of an Arbitrarily Located User

In Figure 3 and Figure 4, we show the simulated achievable rate of an arbitrarily user and compare with the derived asymptotic analytical results in (14-15), as well as the closed-form bounds $R^{B,1}$ in (17) and $R^{B,2}$ in (18). We set $r = 500$ meters. Figure 3 shows the achievable rate for different user location r_u (the distance of the user to the cell center) and path-loss exponent v, while $M = 300$ and $P = 10$dB. Figure 4 shows the achievable rate for different antenna number M and user transmit power P, while $r_u = 300$ meters and $v = 3.6$ [38].

We can see from the figures that the curves numerical calculated by (14-15) accurately predict the simulated ones. The derived closed-form bounds in (17) and (18) are very close to the simulated and numerically calculated achievable rates. The figures show that $R^{B,1}$ is a lower bound and $R^{B,2}$ is an upper bound when $v \geq 4$, while $R^{B,1}$ is an upper bound and $R^{B,2}$ is a lower bound when $v \leq 4$, which confirms the results of (19).

Figure 3 also shows that the achievable rate is higher for larger path-loss exponent and smaller distance between the user distance r_u and the radius of the circular antenna array r. For either $r_u > r$ or $r_u < r$, the achievable rate is a concave function of r_u. We can see from Figure 4 that the achievable rate increases with M. For example, increasing M from 100 to 400 brings an achievable rate increase of about 16% at $P = 10$dB. For the $P = 20$dB case, increasing M from 100 to 400 brings about an achievable rate increase of 12%. The achievable rate also increases with P, the user transmit power. For example, increasing P from 5dB to 20dB results in the achievable rate increase of about 40% at $M = 300$.

B. Average Achievable Rate of the Cell

In Figure 5 and Figure 6, we show the average achievable rate per user of the cell, and compare with the derived bounds $\bar{R}^{B,1}$ in (21) and $\bar{R}^{B,2}$ in (22). We set $r = 500$ meters and
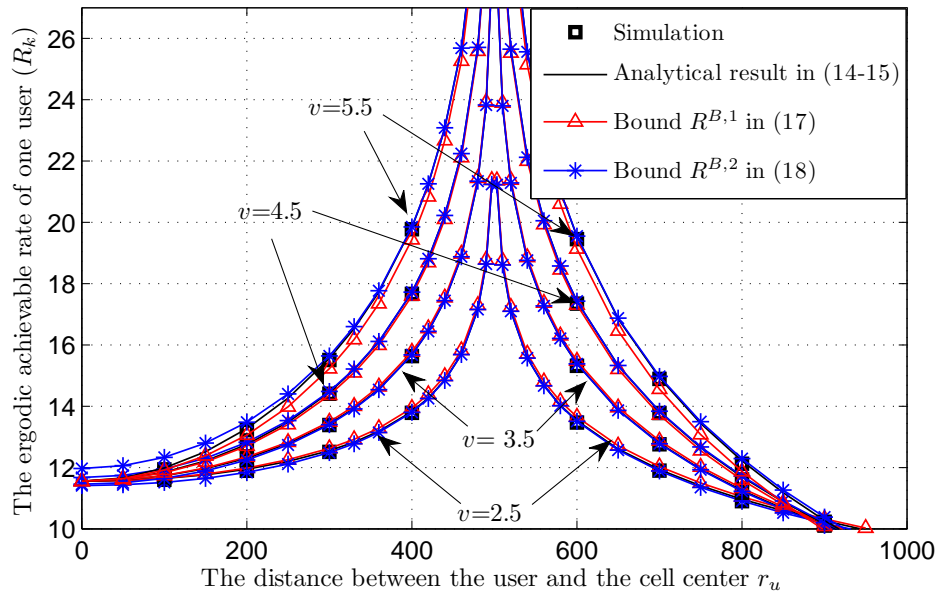
Fig. 3. Comparison of the analytical expressions and bounds of the ergodic achievable rate of distributed massive MIMO with simulation, where $K = 9$, $r = 500$ meters, $M = 300$ and $P = 10$dB.

assume a practical urban scenario with the path-loss exponent $v = 3.6$. The user location are randomly generated to be uniformly distributed in the cell.

It can be seen from both figures that the simulated achievable rate and the derived closed-form bounds match well for all adopted values of M and P. The average achievable rate of the cell increases with M, which indicates that increasing the number of the BS antennas improves the system throughput. For example, the $M = 400$ scenario achieves about 15% higher average rate than the $M = 100$ scenario at $P = 10$dB. The average achievable rate also increases with P. For example, increasing P from 4dB to 14dB brings an achievable rate advantage of about 35% at $M = 100$.

C. Impact of the Location of the Circularly Antenna Array

Next, we show the impart of the radius of circular antenna array, r, on the average achievable rate of the cell. Notice that the $r = 0$ case corresponds to centralized massive MIMO system,
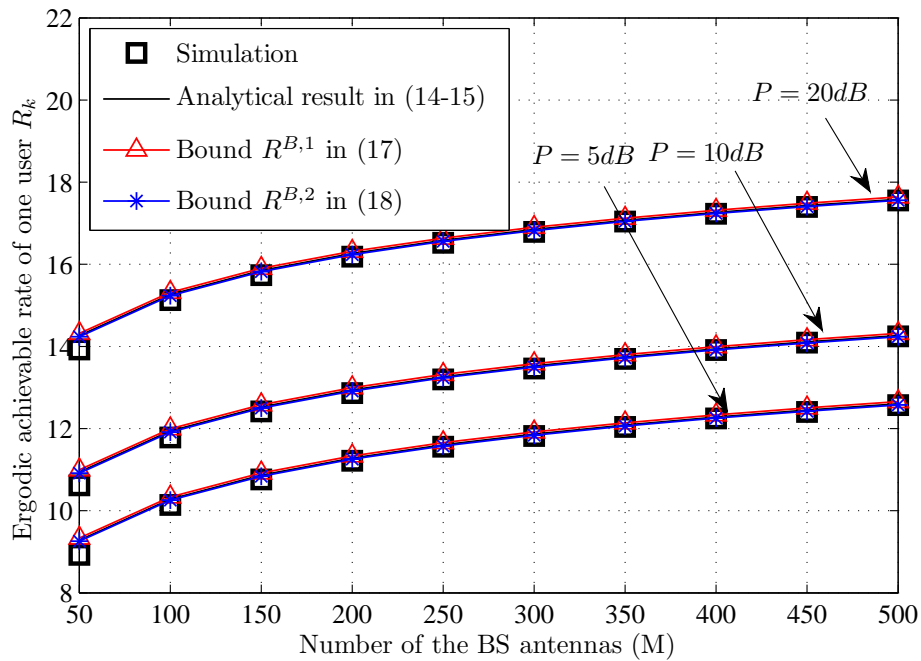
Fig. 4. The ergodic achievable rate of one user for different M where $K = 9$, $r = 500$ meters, $r_u = 300$ meters, and $v = 3.6$.

where the BS antennas are located at the center of the cell.

Figure 7 plots the simulated average rate of the cell and the derived bounds as functions of r for three cases: 1) $M = 150, P = 10$dB, 2) $M = 150, P = 20$dB, and 3) $M = 300, P = 20$dB. We set $v = 3.6$. The figure shows that the radius of the distributed antenna array has significant influence on the average rate of the cell and proper antenna location results in significant improvement in average rate to the centralized case. For example, increasing r from 0 to 750 meters boosts up the average rate by about 30% when $M = 150, P = 20$dB. The figure also indicates that the optimal r for different M and P remains the same, which is about 750 meters. This conforms with our result in Lemma 2 that the optimal r is irrelevant to the values of M and P but only depends on v.

To further understand the optimal radius of the circular antenna array, employing (29) in Lemma 2, we plot r_{opt}/R, the ratio of the optimal antenna array radius to the cell radius, for different path-loss exponent, in Figure 8. It can be seen that r_{opt}/R is bigger for larger v. For
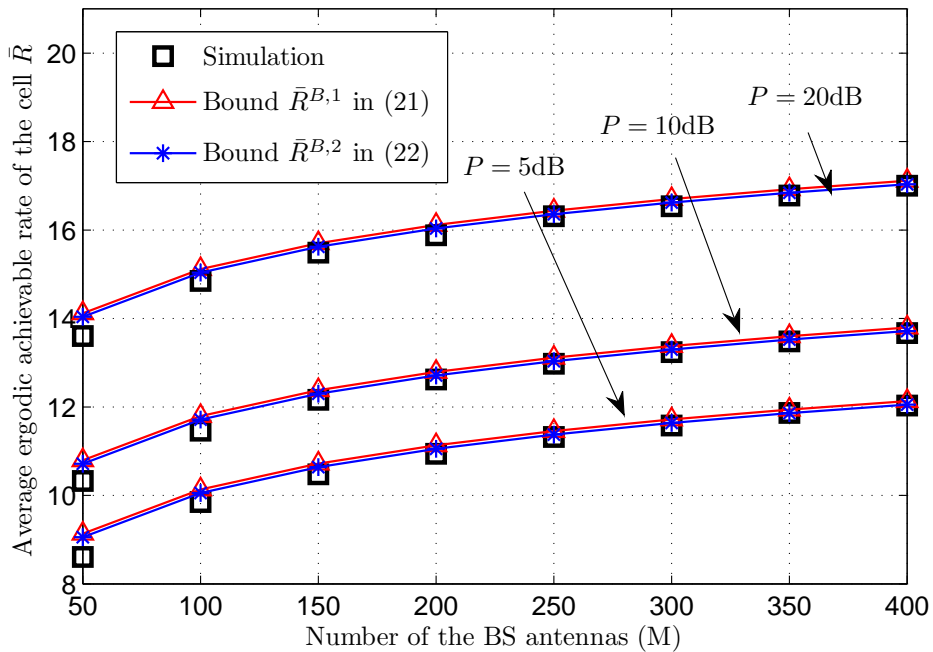
Fig. 5. The average ergodic achievable rate of the cell for different M where $K = 9$, $r = 500$ meters, and $v = 3.6$.

example, when $v = 3.5$, r_{opt}/R is 0.758, while it is 0.766 when $v = 4.0$. Thus, as the path-loss is larger, antennas should be installed further away from the cell center for the maximum average rate. For a given v value, the radius of the circular antennas array should increases linearly in the cell radius R. We can also see that for any $v \in [2, 6]$, $r_{opt}/R \in [0.7, 0.78]$. This shows that the optimal r_{opt}/R value is far away from the centralized massive MIMO case, where $r/R = 0$. On the other hand, for different v values within the practical range ($v \in [2, 6]$), r_{opt}/R has small change. Actually, for any $v \in [2, 6]$, setting the radius of the circular antenna array as $r = 0.75R$ will induce less than 5% loss in the average rate compared to the optimal radius. This result is useful in further simplifying the practical system design of circularly distributed massive MIMO systems.
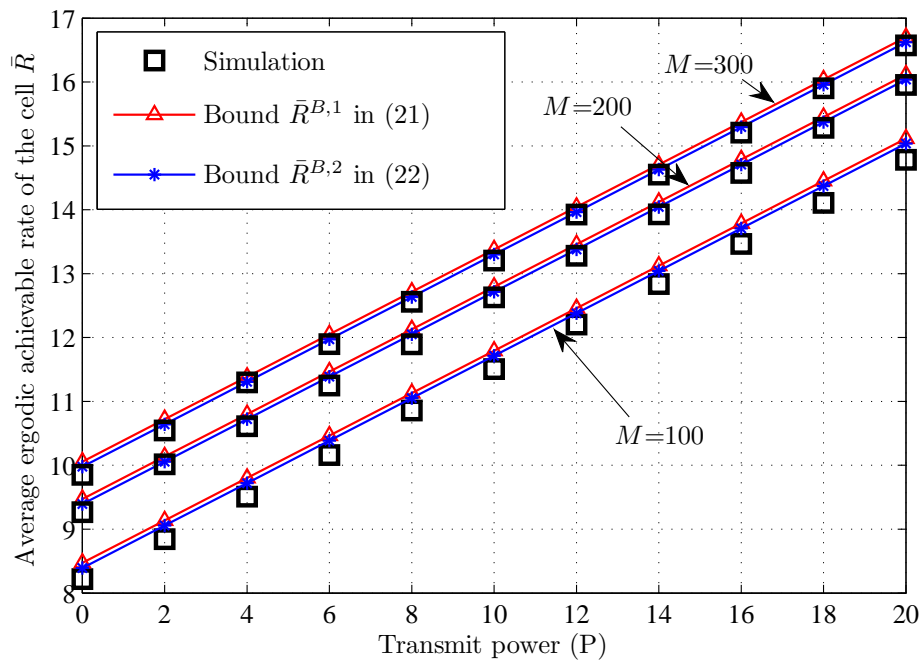
Fig. 6. The average ergodic achievable rate of the cell for different P where $K = 9$, $r = 500$ meters, and $v = 3.6$.

VI. CONCLUSIONS

In this paper, we have considered the uplink of a single-cell multi-user distributed massive MIMO system, where the BS equipped with a large number of distributed antennas receiving information from multiple users equipped with single antenna. Zero-forcing detection is used at the BS. In order to analyze the achievable rate of the system, we provided new results for very long random vectors with independent but non-identically distributed entries. Based on the results, for circularly distributed base station antennas, we derived analytical expressions of the achievable rate of an arbitrarily located user and two closed-form expressions that bound the rate from both sides. The tightness of the bounds were rigorously justified. From these results, behavior of the system achievable rate with respect to different parameters such as the size of the antenna array, the location of the antenna array, the path-loss exponent, and the transmit power can be understood. We also derived tight closed-form bounds for the average achievable rate per user assuming that users are randomly located in the cell, from which the optimal radius
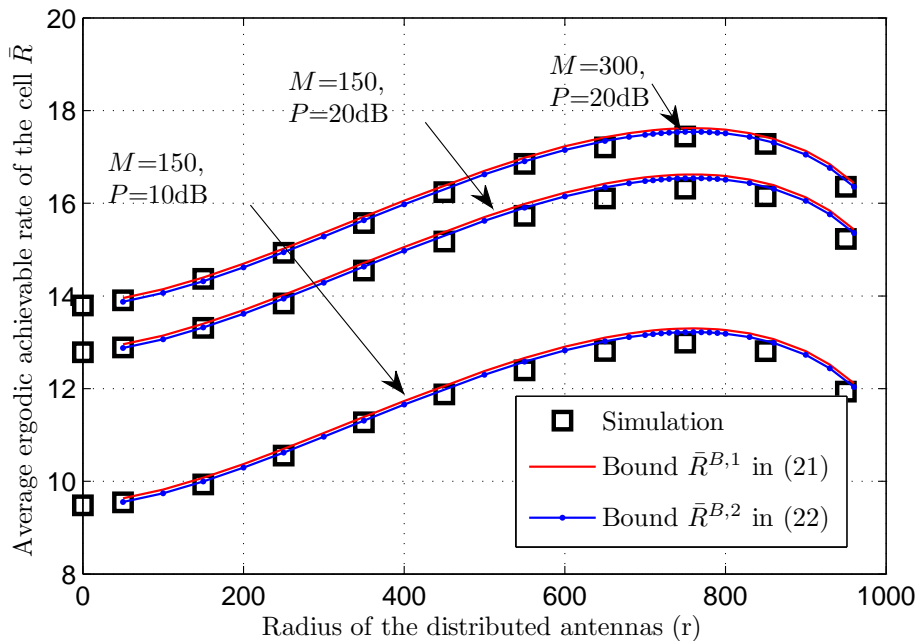
Fig. 7. The average ergodic achievable rate of the cell for different r where $M = 150, P = 10\text{dB}, M = 150, P = 20\text{dB}$, and $M = 300, P = 20\text{dB}$. We set $K = 9$ and $v = 3.6$.

of the distributed antenna array that maximizes the average rate was derived. Numerical results were illustrated to justify our analytical results. Our work has shown that multi-user distributed massive MIMO largely outperforms centralized massive MIMO. Our derived results can assist infrastructure providers in solving the fundamental problems of performance measurement and antennas placement for distributed massive MIMO systems in practice.

APPENDIX A

PROOF OF LEMMA 1

Let $a_i \triangleq |p_i|^2$. Thus a_i's are independent and there exists a finite positive constant C such that

$$\mathbb{E}\{a_i\} = \mathbb{E}\{|p_i|^2\} = \sigma_{p,i}^2, \quad \mathbb{E}\{a_i^2\} = \mathbb{E}\{|p_i|^4\} \leq C. \tag{33}$$
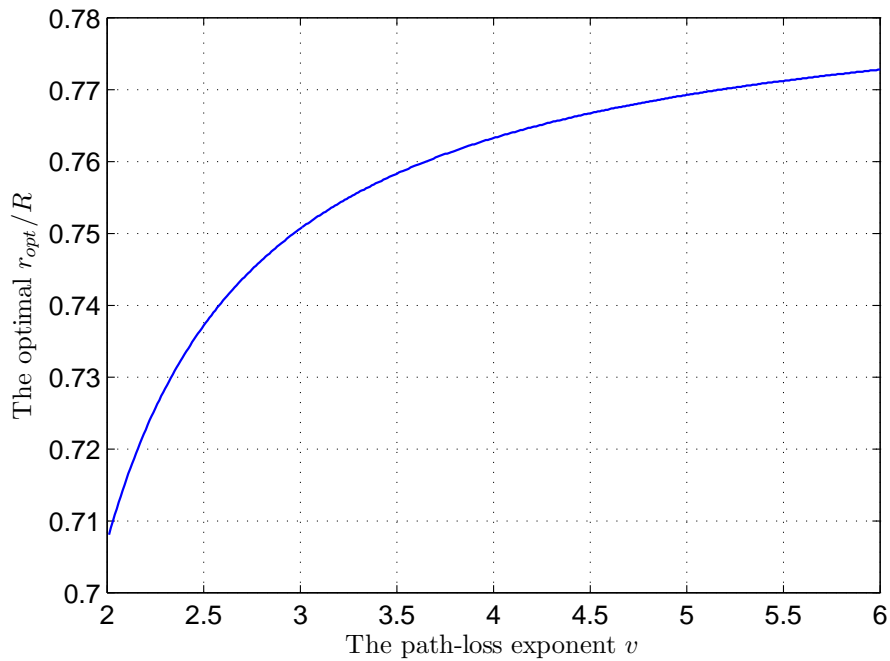
Fig. 8. The relationship between r_{opt}/R and the path-loss exponent v.

The variance of the arithmetic mean of $a_1, a_2, \ldots, a_M$ satisfies the following:

$$Var\left\{\frac{1}{M}\sum_{i=1}^{M}a_i\right\} = \frac{1}{M^2}\sum_{i=1}^{M}Var\{a_i\} \leq \frac{C}{M}. \tag{34}$$

From Chebyshev's inequality, we have

$$\mathbb{P}\left\{\left|\frac{1}{M}\sum_{i=1}^{M}a_i - \frac{1}{M}\sum_{i=1}^{M}\mathbb{E}\{a_i\}\right| < \varepsilon\right\} \geq 1 - \frac{1}{\epsilon^2}Var\left\{\frac{1}{M}\sum_{i=1}^{M}a_i\right\} \geq 1 - \frac{C}{M\varepsilon^2}, \tag{35}$$

where (34) is used in the last step.

From the definition of a_i, we have

$$\frac{1}{M}\mathbf{p}^H\mathbf{p} = \frac{1}{M}\sum_{i=1}^{M}|p_i|^2 = \frac{1}{M}\sum_{i=1}^{M}a_i. \tag{36}$$

Using this in (35), we obtain

$$1 \geq \mathbb{P}\left\{\left|\frac{1}{M}\mathbf{p}^H\mathbf{p} - \frac{1}{M}\sum_{i=1}^{M}\sigma_{p,i}^2\right| < \varepsilon\right\} \geq 1 - \frac{C}{M\varepsilon^2}. \tag{37}$$

When $M \to \infty$, $1 - \frac{C}{M\varepsilon^2} \to 1$. Thus, Eq. (6) is proved.

Since p_i and q_i are independent, we have $\mathbb{E}\left\{p_i^H q_i\right\} = 0$, $i = 1, 2, \ldots, M$. Following the same arguments in the proof of (6), Eq. (7) can be proved.

APPENDIX B

PROOF OF THEOREM 3

As shown in Figure 2, we use O for the cell center. To help the derivation, we denote the angle of the segments OT_m (where T_m is the location of the mth BS antenna) and OU (where U is the location of the user) as α_m. The distance between T_M and U, denoted as D_m, can be expressed as

$$D_m = \sqrt{r^2 \sin^2 \alpha_m + (r \cos \alpha_m - r_u)^2}. \tag{38}$$

Without loss of generality, we assume that $\alpha_1 = 0$ and the evenly circularly distributed BS antennas are labeled such that $\alpha_m = \frac{m-1}{M} 2\pi$ for $1 \leq m \leq \lfloor \frac{M}{2} \rfloor$ and $\alpha_m = \left(\frac{m-1}{M} - 1\right) 2\pi$ for $\lceil \frac{M}{2} \rceil \leq m \leq M$. Let $\Delta\alpha \triangleq \frac{2\pi}{M}$.

From Eqs. (2) and (38),

$$\frac{1}{M} \sum_{m=1}^{M} \beta_{mk} = \frac{1}{M} \sum_{m=1}^{M} \frac{1}{D_m^v}$$

$$= \frac{1}{M} \sum_{m=1}^{M} \left[r^2 \sin^2 \alpha_m + (r \cos \alpha_m - r_u)^2\right]^{-\frac{v}{2}} \tag{39}$$

$$= \frac{1}{M} \frac{1}{\Delta\alpha} \sum_{m=1}^{M} \left[r^2 \sin^2 \alpha_m + (r \cos \alpha_m - r_u)^2\right]^{-\frac{v}{2}} \Delta\alpha \tag{40}$$

$$\xrightarrow{M \to \infty} \frac{1}{2\pi} \int_{-\pi}^{\pi} \left[r^2 \sin^2 \alpha + (r \cos \alpha - r_u)^2\right]^{-\frac{v}{2}} d\alpha. \tag{41}$$

Employing [39, 2.5.16.38], we have, from (41),

$$\frac{1}{M} \sum_{m=1}^{M} \beta_{mk} \xrightarrow{M \to \infty} \left|r^2 - r_u^2\right|^{-\frac{v}{2}} P_{\frac{v}{2}-1}\left(\frac{r^2 + r_u^2}{|r^2 - r_u^2|}\right). \tag{42}$$

By using (42) in (8), Eq. (14) can be proved. Eq. (16) can be subsequently obtained by using Eq. [37, 8.912].

To further illuminate the asymptotic result in (41), we investigate the difference between (41) and (40). To help the presentation, we use the following notation:

$$f(\alpha) \triangleq \left[r^2 \sin^2 \alpha + (r \cos \alpha - r_u)^2 \right]^{-\frac{v}{2}}.$$

For $\alpha \in [0, \pi]$, we can obtain via straightforward calculations that

$$\frac{\partial f}{\partial \alpha} = -v \left[r^2 \sin^2 \alpha + (r \cos \alpha - r_u)^2 \right]^{-\frac{v}{2}-1} r r_u \sin \alpha \leq 0. \tag{43}$$

This shows that f decreases with α when $\alpha \in [0, \pi]$. For the simplicity of presentation, we assume that M is even. The proof for odd M is similar. The difference between (41) and (40) can be bounded as follows:

$$I_{diff} \triangleq \frac{1}{M\Delta\alpha} \sum_{m=1}^{M} \left[r^2 \sin^2 \alpha_m + (r \cos \alpha_m - r_u)^2 \right]^{-\frac{v}{2}} \Delta\alpha - \frac{1}{2\pi} \int_{-\pi}^{\pi} f(\alpha) \, d\alpha \tag{44}$$

$$= 2 \frac{1}{M\Delta\alpha} \sum_{m=1}^{\frac{M}{2}} \left[r^2 \sin^2 \alpha_m + (r \cos \alpha_m - r_u)^2 \right]^{-\frac{v}{2}} \Delta\alpha - \frac{1}{2\pi} \int_{0}^{\pi} f(\alpha) \, d\alpha \tag{45}$$

$$= \frac{1}{\pi} \sum_{m=1}^{\frac{M}{2}} f_k \left(\frac{m-1}{M} 2\pi \right) \frac{2\pi}{M} - \sum_{m=1}^{\frac{M}{2}} \int_{\frac{m-1}{M}}^{\frac{m}{M}} f(\alpha) \, d\alpha \tag{46}$$

$$\leq \frac{1}{\pi} \sum_{m=1}^{\frac{M}{2}} \left[f \left(\frac{m-1}{M} 2\pi \right) - f \left(\frac{m}{M} 2\pi \right) \right] \frac{2\pi}{M} \tag{47}$$

$$= \frac{2}{M} [f(0) - f(\pi)] = \frac{2}{M} \left[(r - r_u)^{-v} - (r + r_u)^{-v} \right] \overset{M \to \infty}{\longrightarrow} 0. \tag{48}$$

In obtaining (45), we use the symmetry in $f(\alpha)$. This analysis shows that the difference between (41) and (40) is linear in $1/M$. For large but finite number of antennas, (41) is a tight approximation of (40).

APPENDIX C

PROOF OF THEOREM 4

Define $z \triangleq \frac{r^2 + r_u^2}{|r^2 - r_u^2|}$. Notice that $z \geq 1$ always. Using [37, 8.882.1], we have

$$P_{\frac{v}{2}-1} \left(\frac{r^2 + r_u^2}{|r^2 - r_u^2|} \right) = P_{\frac{v}{2}-1}(z)$$

$$= \frac{1}{\pi} \int_0^\pi \left(z + \sqrt{z^2 - 1} \cos \varphi \right)^{\frac{v}{2} - 1} d\varphi$$

$$= \frac{z^{\frac{v}{2} - 1}}{\pi} \int_0^\pi \left(1 + \frac{\sqrt{z^2 - 1}}{z} \cos \varphi \right)^{\frac{v}{2} - 1} d\varphi$$

$$= \frac{z^{\frac{v}{2} - 1}}{\pi} \int_0^{\frac{\pi}{2}} \left(1 + \frac{\sqrt{z^2 - 1}}{z} \cos \varphi \right)^{\frac{v}{2} - 1} d\varphi + \frac{z^{\frac{v}{2} - 1}}{\pi} \int_{\frac{\pi}{2}}^\pi \left(1 + \frac{\sqrt{z^2 - 1}}{z} \cos \varphi \right)^{\frac{v}{2} - 1} d\varphi$$

$$= \frac{z^{\frac{v}{2} - 1}}{\pi} \int_0^{\frac{\pi}{2}} \underbrace{\left[\left(1 + \frac{\sqrt{z^2 - 1}}{z} \cos \varphi \right)^{\frac{v}{2} - 1} + \left(1 - \frac{\sqrt{z^2 - 1}}{z} \cos \varphi \right)^{\frac{v}{2} - 1} \right]}_{g(v, z, \varphi)} d\varphi. \tag{49}$$

Next, we look for bounds for $g(v, z, \varphi)$. We derive the derivative of $g(v, z, \varphi)$ with respect to z as follows:

$$\frac{\partial}{\partial z} g(v, z, \varphi)$$

$$= \frac{\frac{v}{2} - 1}{z^2 \sqrt{z^2 - 1}} \left[\left(1 + \frac{\sqrt{z^2 - 1}}{z} \cos \varphi \right)^{\frac{v}{2} - 2} - \left(1 - \frac{\sqrt{z^2 - 1}}{z} \cos \varphi \right)^{\frac{v}{2} - 2} \right] \cos \varphi. \tag{50}$$

Since $z \geq 1$, we have $\sqrt{z^2 - 1}/z \in [0, 1]$. Thus for $\varphi \in [0, \frac{\pi}{2}]$,

$$\begin{cases} \frac{\partial}{\partial z} g(v, z, \varphi) \leq 0 & \text{when } v \leq 4 \\ \frac{\partial}{\partial z} g(v, z, \varphi) \geq 0 & \text{when } v \geq 4 \end{cases}.$$

We can subsequently bound $g(v, z, \varphi)$ as follows:

$$\begin{cases} g(v, \infty, \varphi) \leq g(v, z, \varphi) \leq g(v, 1, \varphi) & \text{when } 2 \leq v \leq 4 \\ g(v, 1, \varphi) \leq g(v, z, \varphi) \leq g(v, \infty, \varphi) & \text{when } 6 \geq v \geq 4 \end{cases}. \tag{51}$$

Define

$$B_1 \triangleq \frac{z^{\frac{v}{2} - 1}}{\pi} \int_0^{\frac{\pi}{2}} g(v, 1, \varphi) d\varphi$$

$$= \frac{z^{\frac{v}{2} - 1}}{\pi} \int_0^{\frac{\pi}{2}} \left[(1 + 0 \times \cos \varphi)^{\frac{v}{2} - 1} + (1 - 0 \times \cos \varphi)^{\frac{v}{2} - 1} \right] d\varphi = z^{\frac{v}{2} - 1}.$$

$$B_2 \triangleq \frac{z^{\frac{v}{2} - 1}}{\pi} \int_0^{\frac{\pi}{2}} g(v, \infty, \varphi) d\varphi$$

$$= \frac{z^{\frac{v}{2} - 1}}{\pi} \int_0^{\frac{\pi}{2}} \left[(1 + \cos \varphi)^{\frac{v}{2} - 1} + (1 - \cos \varphi)^{\frac{v}{2} - 1} \right] d\varphi$$

$$= \frac{z^{\frac{v}{2} - 1}}{\pi} \int_0^\pi (1 + \cos \varphi)^{\frac{v}{2} - 1} d\varphi = \frac{z^{\frac{v}{2} - 1}}{\pi} \int_0^\pi 2^{\frac{v}{2} - 1} \cos^{v - 2} \left(\frac{\varphi}{2} \right) d\varphi$$

$$= \frac{z^{\frac{v}{2}-1}}{\pi} \int_0^{\frac{\pi}{2}} 2^{\frac{v}{2}} \cos^{v-2}(t)\, dt = \frac{2^{3\left(\frac{v}{2}-1\right)} \Gamma^2 \left(\frac{v}{2}-\frac{1}{2}\right)}{\pi \Gamma(v-1)} z^{\frac{v}{2}-1}. \tag{52}$$

The last step is obtain by using [37, 3.621.1] and [37, 8.384.1].

From (49) and (51), $P_{\frac{v}{2}-1}(z)$ can be bounded as:

$$\begin{cases} B_1 \geq P_{\frac{v}{2}-1}(z) \geq B_2 & \text{when } 2 \leq v \leq 4 \\ B_1 \leq P_{\frac{v}{2}-1}(z) \leq B_2 & \text{when } 6 \geq v \geq 4 \end{cases}. \tag{53}$$

By applying (53) in (15) and (14), the first two lines of (19) can be obtained. For the special cases of $\nu = 2, 4$, with the aid of Eq. [37, 8.338.2], $\Gamma(1/2) = \sqrt{\pi}$, $\Gamma(3/2) = \sqrt{\pi}/2$, we have $\frac{2^{\frac{3}{2}v-3} \Gamma^2 \left(\frac{v}{2}-\frac{1}{2}\right)}{\pi \Gamma(v-1)} = 1$. The two bounds are equal. Thus the last line of (19) is proved.

REFERENCES

[1] A. Osseiran, F. Boccardi, V. Braun, K. Kusume, P. Marsch, M. Maternia, O. Queseth, M. Schellmann, H. Schotten, H. Taoka, H. Tullberg, M. A. Uusitalo, B. Timus, and M. Fallgren, "Scenarios for 5G mobile and wireless communications: the vision of the METIS project," *IEEE Commun. Mag.,* vol. 52, no. 5, pp. 26-35, May. 2014.

[2] V. Jungnickel, K. Manolakis, W. Zirwas, B. Panzner, V. Braun, M. Lossow, M. Sternad, R. Apelfr ojd, and T. Svensson, "The role of small cells, coordinated multipoint, and massive MIMO in 5G," *IEEE Commun. Mag.,* vol. 52, no. 5, pp. 44-51, May. 2014.

[3] E. Telatar, "Capacity of multi-antenna Gaussian channels," *Europ. Trans. on Telecomm.*, vol. 10, no. 6, pp. 585–596, Nov. 1999.

[4] A. Sibille, C. Oestges, and A. Zanella. *MIMO: from theory to implementation*. Academic Press, 2010.

[5] H. Liu, Y. Zhang and J. Luo, *Distributed Antenna Systems: Open Architecture for Future Wireless Communications.* Auerbach Publication, 2007.

[6] H. Zhu, S. Karachontzitis, and D. Toumpakaris, "Low complexity resource allocation and its application to distributed antenna systems," *IEEE Wireless Commun. Mag.,* vol. 17, no. 3, pp. 44–50 Jun. 2010.

[7] W. Roh, "High performance distributed antenna cellular networks," *Ph.D. Thesis*, Stanford Univ., 2003.

[8] J. Wang, H. Zhu, and N. J. Gomes "Distributed antenna systems for mobile communications in high speed trains," *IEEE J. Sel. Areas Commun.*, vol. 30, no. 4, pp. 675-683, May 2012.

[9] W. Roh and A. Paulraj, "Outage performance of the distributed antenna systems in a composite fading channel," in *Proc. IEEE Veh. Technol. Conf. (VTC) Fall*, vol. 3, Sept. 2002.

[10] L. Dai, "A comparative study on uplink sum capacity with co-Located and distributed antennas," *IEEE J. Sel. Areas Commun.*, vol. 29, no. 6, pp. 1200-1213, Jun. 2011.

[11] E. Park, S.-R. Lee, and I. Lee, "Antenna placement optimization for distributed antenna systems," *IEEE Trans. Wireless Commun.,* vol. 11, no. 7, pp. 2468-2477, Jul. 2012.

[12] H. Zhu and J. Wang, "Radio resource allocation in multiuser distributed antenna systems," *IEEE J. Sel. Areas Commun.*, vol. 31, no. 10, pp. 2058-2066, Oct. 2013.

[13] T. Wu and P. Hosein, "Radio resource management strategies for distributed antenna systems," in *Proc. IEEE Wireless Commun. Netw. Conf. (WCNC)*, Apr. 2010.

[14] W. Feng, Y. Wang, N. Ge, J. Lu, and J. Zhang, "Virtual MIMO in multi-cell distributed antenna systems: Coordinated transmissions with large-scale CSIT," *IEEE J. Sel. Areas Commun.*, vol. 31, no. 10, pp. 2067-2081, Oct. 2013.

[15] T. L. Marzetta, "Noncooperative cellular wireless with unlimited numbers of base station antennas", *IEEE Trans. wireless Commun.*, vol. 9, no. 11, pp. 3590-3600, Nov. 2010.

[16] C. Artigue, P. Loubaton, "On the precoder design of flat fading MIMO systems equipped with MMSE receivers: A large system approach," *IEEE Trans. Inform. Theory*, vol. 57, no. 7, pp. 4138-4155, Jul. 2011.

[17] A. Pitarokoilis, S. K. Mohammed, and E. G. Larsson, "On the optimality of single-carrier transmission in large-scale antenna systems," *IEEE Wireless Commun. Lett.*, vol. 1, no. 4, pp. 276-279, Aug. 2012.

[18] H. Huh, G. Caire, H. C. Papadopoulos, and S. A. Ramprashad, "Achieving massive MIMO spectral efficiency with a not-so-large number of antennas," *IEEE Trans. Wireless Commun.*, vol. 11, no. 9, pp. 3226-3239, Sep. 2012.

[19] F. Rusek, D. Persson, B. K. Lau, E. G. Larsson, T. L. Marzetta, O. Edfors, and F. Tufvesson, "Scaling up MIMO: Opportunities and challenges with very large arrays," *IEEE Sig. Proc. Mag.*, vol. 30, no. 1, pp. 40-46, Jan. 2013.

[20] H. Q. Ngo, E. G. Larsson, and T. L. Marzetta, "Energy and spectral efficiency of very large multiuser MIMO systems," *IEEE Trans. Commun.*, vol. 61, no. 4, pp. 1436-1449, Apr. 2013.

[21] J. Hoydis, S. ten Brink, and M. Debbah, "Massive MIMO in UL/DL cellular systems: How many antennas do we need?" *IEEE J. Sel. Areas Commun.*, vol. 31, no. 2, pp. 160-171, Feb. 2013.

[22] H. Yang and T. L. Marzetta, "Performance of conjugate and zero-forcing beamforming in large-scale antenna systems," *IEEE J. Sel. Areas Commun.*, vol. 31, no. 2, pp. 172-179, Feb. 2013.

[23] F. Fernandes, A. Ashikhmin, and T. L. Marzetta, "Inter-cell interference in noncooperative TDD large scale antenna systems," *IEEE J. Sel. reas Commun.*, vol. 31, no. 2, pp. 192-201, Feb. 2013.

[24] R. Aggarwal, C. E. Koksal, and P. Schniter, "On the design of large scale wireless systems," *IEEE J. Sel. reas Commun.*, vol. 31, no. 2, pp. 215-225, Feb. 2013.

[25] H. Q. Ngo, E. G. Larsson, and T. L. Marzetta, "The multicell multiuser MIMO uplink with very large antenna arrays and a finite-dimensional channel," *IEEE Trans. Commun.*, vol. 61, no. 6, pp. 2350-2361, Jun. 2013.

[26] T. Datta, N. A. Kumar, A. Chockalingam, and B. S. Rajan, "A novel Monte Carlo sampling based receiver for large-scale uplink multiuser MIMO systems," *IEEE Trans. Veh. Technol.*, vol. 62, no. 7, pp. 3019-3038, Sep. 2013.

[27] J. Zhang, C.-K. Wen, S. Jin, X. Gao, and K.-K. Wong, "On capacity of large-scale MIMO multiple access channels with distributed sets of correlated antennas," *IEEE J. Sel. Areas Commun.*, vol. 31, no. 2, pp. 133-148, Feb. 2013.

[28] M. Matthaiou, C. Zhong, M. R. McKay, and T. Ratnarajah, "Sum rate analysis of ZF receivers in distributed MIMO systems" *IEEE J. Sel. Areas Commun.*, vol. 31, no. 2, pp. 180-191, Feb. 2013.

[29] A. Ozgur, O. Leveque, and D. Tse, "Spatial degrees of freedom of large distributed MIMO systems and wireless ad hoc networks," *IEEE J. Sel. Areas Commun.*, vol. 31, no. 2, pp. 202-214, Feb. 2013.

[30] H. Yin, D. Gesbert, L. Cottatellucci, "Dealing with interference in distributed large-scale MIMO systems: a statistical approach," to appear on *IEEE J. Sel. Topics Signal Process.*, 2014. [Online]. Available: http://arxiv.org/abs/1310.6674.

[31] J. Joung, Y. K. Chia, and S. Sun, "Energy-efficient, large-scale distributed-antenna system (L-DAS) for multiple users," to appear on *IEEE J. Sel. Topics Signal Process.*, 2014. [Online]. Available: http://arxiv.org/abs/1312.1870.

[32] W. Feng, X. Xu, S. Zhou, J. Wang, and M. Xia, "Sum rate characterization of distributed antenna systems with circular antenna layout," in *Proc. IEEE 69th Veh. Technol. Conf. (VTC) Spring*, Apr. 2009.

[33] S. Firouzabadi and A. Goldsmith, "Optimal placement of distributed antennas in cellular systems," in *Proc. IEEE 21th Signal Processing Advances in Wireless Communications (SPAWC)*, Jun. 2011.

[34] L. Han, Y. Tang, S. Shao, and T. Wu, "On the design of antenna location for OSTBC with distributed transmit antennas in a circular cell," in *Proc. IEEE International Conference on Communications (ICC)*, May. 2010.

[35] S. Cui, A. J. Goldsmith, and A. Bahai, "Energy-efficiency of MIMO and cooperative MIMO techniques in sensor networks" *IEEE J. Sel. Areas Commun.*, vol. 22, no. 6, pp. 1089-1098, Aug. 2004.

[36] W. Choi and J. Y. Kim, "Forward-link capacity of a DS/CDMA system with mixed multirate sources" *IEEE Trans. Veh. Technol.*, vol. 50, no. 3, pp. 737-749, May 2001.

[37] I. S. Gradshteyn and I. M. Ryzhik, *Table of Integrals, Series, and Products, 7th Ed.* Academic Press, New York, 2007.

[38] D. Tse and P. Viswanath, *Fundamentals of Wireless Communication*. Cambridge University Press, 2005.

[39] A. P. Prudnikov, Y. A. Brychkov, and O. I. Marichev, *Integrals and Series, Volume 1: Elementary Functions*. Gordon and Breach Science Publishers, 1986.